UNIVERSITY OF CALIFORNIA,

IRVINE

Reliability Analysis of Steel SMRF and SCBF Structures considering the Vertical Component of Near-Fault Ground Motions

THESIS

submitted in partial satisfaction of the requirements
for the degree of

MASTER OF SCIENCE
in Civil Engineering

by

Jawad Fayaz

Thesis Committee:

Associate Professor Farzin Zareian, Chair
Professor Farzad Naeim
Professor Lizhi Sun

2018

DEDICATION

To my parents and brothers in recognition of the incredible amount of effort they have employed to support my graduate dream emotionally and financially, especially to my mother, Shahzana, who has been an unconditional source of encouragement through all transitions of my life. And without hesitation, to my ingenious advisor and mentor, Dr. Farzin Zareian, in recognition of the profuse amount of time dedicated to my academic development and for patiently tolerating my mistakes (which I am sure were many instances) and lastly for being such an amazing inspiration.

"Greatness doesn`t come overnight. It comes one step at a time"

-Tricia Downing

TABLE OF CONTENTS

LIST OF FIGURES

LIST OF TABLES

ACKNOWLEDGEMENTS

There are many people who have walked alongside me during this graduate program. Fore mostly I would like to express deepest gratitude and gratefulness to my thesis advisor and committee chair Dr. Farzin Zareian, who has been nothing less than an inspiration for me since the onset of my graduate program. His implausible intelligence, incredible tenacity and great acumen for outstanding research are a tremendous source of motivation for me to pursue my career goals in this field of science. Also, his wittiness and friendliness made my journey of master`s program full of delight and enjoyment. It would be an understatement to say that I couldn't ask for a better advisor. It has been an honor and a privilege to be his student and I thank him for allowing me the opportunity to work with him.

I would also like to thank Dr. Farzad Naeim for sharing his opinions and constructive criticism throughout the course of this study. Also, being a part of his class for two earthquake engineering related courses was an astounding experience. Without his diligent teaching methods and sharing parts of his plethora of knowledge, the research presented herein would not have been possible. I also thank my committee member Dr. Lizhi Sun for agreeing to be a part of my thesis committee and motivating me through his keen research work.

I would also like to thank all my friends for supporting me, especially Nitish Nayak, who guided me through the right doors of coding and programming, without which this research would have been a lot more tiring journey. Lastly, I thank God, for always being with me and providing me with right people at the right times of my career to guide me.

ABSTRACT OF THE THESIS

Reliability Analysis of Steel SMRF and SCBF Structures considering the Vertical Component of Near-Fault Ground Motions

By

Jawad Fayaz

Master of Science in Civil Engineering

University of California, Irvine, 2018

Professor Farzin Zareian, Chair

The current US seismic design codes are believed to do no justice to signify the effects of vertical component of ground motions. This study assesses the effects of the vertical component of ground motions on steel structures and evaluates the current seismic design provisions of ASCE 7 based on a structural reliability outlook. Eight SMRF and SCBF steel structures are analyzed under two groups of near-fault (i.e. strike-slip and reverse fault) ground motions. Detailed methodology for calculating the Reliability Index (β) of structural components is explained; β is computed for structural component actions including moment & shear in beams, axial load in braces, and axial load and moment in columns. Seismic provisions of ASCE 7 were developed with an intention to achieve target β of 1.75 for earthquake-resistant structural members. Results indicate that the implementation of current seismic load combinations, in which a load factor equal to 20% of design level short period spectral acceleration on structural dead load is used to account for the effects of the vertical component of ground motions, results in $\beta \sim 1.3$ for most structural members. Application of structural system drift limits, however, results in increased member sizes in SMRFs by which β values larger than 1.75 are achieved. It is concluded that current seismic load combinations in ASCE 7 are inadequate to account for the effects of the vertical component of near-fault ground motions. Nevertheless, performance-based design provisions can provide a reasonable and adequate margin of safety against structural member failure.

CHAPTER 1

INTRODUCTION

1.1. Background

The vertical component of ground motions is dominated by vertically propagating compression waves (P-waves) and have different physical characteristics than the conventionally prioritized horizontal ground motions which are subjugated by shear waves (S-waves). P-waves have a shorter wavelength than S-waves, therefore, the vertical component of ground motions have a higher frequency content as compared to the horizontal component (Kim *et al.*, 2011). The vertical component of ground motions may have a detrimental impact on building structures, however, neither practitioners nor researchers have paid significant attention to account for the effects of such excitations on building structures. One of the earlier methods to capture these effects was proposed for the design of nuclear power plants by Newmark (1973) in which vertical response spectrum was anticipated as two-thirds of the horizontal design spectrum. This implies that the ratio of vertical to horizontal spectra (V/H) is constant (i.e. equal to 2/3) over all periods, site-to-source distances, site conditions and frequencies (Bozorgnia *et al.*, 2003; Bozorgnia *et al.*, 1995). Recent studies as well as ground motion recordings, however, have shown that V/H is not constant and depends on the target period, site location, and site condition. In addition, newly developed V/H ground motion attenuation relationships signify the difference between the vertical spectra and horizontal spectra depending on the distance, magnitude, site, and other conditions (Bozorgnia *et al.*, 2016).

Minimum Design Loads for Buildings and Other Structures (ASCE 7-10, 2010; ASCE 7-16, 2016)–denoted as ASCE 7 for simplicity–provides mapped risk-targeted maximum considered earthquake in the form of short period and 1-second spectral accelerations. The design spectrum is constructed using these two values. These mapped spectral acceleration values are based on achieving 1% probability of collapse within a 50-year period. Due to the higher frequency content of the vertical component of seismic excitation, ASCE 7 quantifies the effect of the vertical component of ground motions in terms of 20% of short-period design value spectral acceleration, S_{DS}. This factor is only used at sites where S_{DS} < 0.125g, otherwise the vertical component is deemed insignificant. ASCE 7 suggests $(1.2 + 0.2S_{DS})D_n + \rho E_n + 0.5L_n$ and $(0.9 - 0.2S_{DS})D_n + \rho E_n + 0.5L_n$ as load combinations to incorporate the effect of vertical component of ground motions. In these two equations, D_n is the nominal Dead Load, ρ is the Redundancy Factor (equals to 1 or 1.3 depending on the load path of lateral force system), E_n signifies the nominal horizontal seismic forces (which are calculated by Response Spectrum Analysis) and L_n represents the nominal "arbitrary-point-in-time" Live Load acting on the structure.

The present load criteria of ASCE 7 has evolved from American National Standard A58 (ANSI A58 8.1-1980) by Ellingwood *et al.* (1980), which incorporated the probabilistic limit state design and led to Load and Resistance Factor Design (LRFD) methodology. ANSI A58 8.1-1980 was based on a hazard level of 10% in 50 years (Return Period of 475 years) and didn`t take the vertical component of ground motions into consideration. The seismic load combinations adopted by this code were $1.2D_n + 1.5E_n + 0.5L_n$ and $0.9D_n - 1.5E_n$. Due to the random nature of resistance and load effects, the development of these load combinations was performed under the context of Reliability Based Design. Current design codes regard component reliability to be synonymous

with system reliability. Within this backdrop, reliability of a component (and therefore structure's reliability) in simple terms is defined as probability of no failure of any component, where failure is said to happen when the component passes any of its defined limit states (Ellingwood *et al.*, 1980).

Reliability of a structure is expressed in terms of "Reliability" or "Safety" Index (β). In this approach, the load and resistance terms are assumed to be random variables and with all the necessary statistical information a limit state equation is formed. Per Ellingwood *et al.* (1980) recommendation, consider a limit state equation of $Z = R - S$, where R represents the random variable for resistance and S is the random variable representing loads. Assuming R and S are independent random variables, the failure is observed whenever random variable S takes a greater value than R and the probability of failure (p_f) can be computed as shown in Eq. (1). In this equation F_R is the Cumulative Probability Distribution Function (*CDF*) of R and f_S is the Probability Density Function (*PDF*) for S. Using the Mean-Value-First-Order-Second-Moment approach, an approximation of the probability of failure (p_{f1}) is computed using Eq. (2) where μ_R and σ_R are the mean and standard deviation for R and μ_S and σ_S are the mean and standard deviation for S and $\Phi[.]$ represents the standard normal probability distribution. Mean and standard deviation of limit state function Z can be expressed as $\mu_Z = \mu_R - \mu_S$ and $\sigma_Z = \sqrt{{\sigma_R}^2 + {\sigma_S}^2}$, respectively and the Mean-Value-First-Order-Second-Moment reliability index, β_{MVFOSM}, can be defined as shown in Eq. (3).

$$p_f = \text{p (R < S)} = \int_0^\infty F_R(x) f_S(x) dx \quad (1)$$

$$p_{f1} = \Phi\left[-\frac{\mu_R - \mu_S}{\sqrt{{\sigma_R}^2 + {\sigma_S}^2}}\right] \quad (2)$$

$$\beta_{MVFOSM} = \frac{\mu_R - \mu_S}{\sqrt{\sigma_R{}^2 + \sigma_S{}^2}} = \frac{\mu_Z}{\sigma_Z} \quad (3)$$

β_{MVFOSM} is invariant to different mechanically equivalent formulations of the same problem (e.g. when loads counteract each other) and does not appreciate the probability distribution function associated with *R* and *S* (Ellingwood *et al.*, 1980; Thoft-Christensen *et al.*, 1982). To alleviate this caveat, First Order Reliability Method (FORM) is used in this study to calculate the reliability index of structural components (β_{FORM}). Calculation of β_{FORM} is an iterative process in which the probability distribution function of *R* and *S* are utilized to estimate the so-called "design point" where limit state function $Z = 0$. The latter represents a point on the limit state function that has the largest likelihood of failure (Melchers, 1999; Hasofer *et al.*, 1974; Der Kiureghian *et al.* 1986). For simplicity of presentation, we denoted β as the equivalent of β_{FORM}.

Reliability-Based Design involves the selection of load and resistance factors (code calibration) that produce desired level of uniformity in the probability of safety (probability of no failure), hence uniformity in reliability index. For enabling intelligent selection of the load and resistance factors, the codes are calibrated to obtain certain levels of 'Target Reliability' (denoted as β_T), which are set independently for each load combination depending on the type of load and material. These range from $\beta_T = 1.5$ for some tension members to over $\beta_T = 7$ for certain masonry walls (Ellingwood *et al.*, 1980). For steel and concrete structures, $\beta_T = 3.0$ is set for load combinations including only gravity loads, while $\beta_T = 2.5$ is selected for load combinations including wind loads. Given the high variability in earthquake loads, load combinations incorporating Earthquake Load have a $\beta_T = 1.75$ (probability of failure within 50-year lifetime ≈ 4%). The load and resistance factors are then calibrated accordingly to attain the assigned β_T.

1.2. Intro to study

This study assesses β values for various members of common steel structures in high seismic areas. It shows old and new code calibrations and how vertical component of ground motions affects the values of β in different structural members. The study aims to derive the statistical information of loads and resistance (i.e. random variables) of various components and then develop a simplified procedure to calculate their reliability index. The study was conducted on steel structures; specifically, on Special Moment Resisting Frame (SMRF) and Special Concentric Braced Frame (SCBF) buildings. The results are primarily deduced from the analysis of beams, columns, and braces of the lateral load resistant system and not the Gravity system of the designed buildings. The evaluation is based on unscaled linear time history analysis of structures under 2 groups (depending on the type of fault) of near-fault ground motions, with each group consisting of 30 sets of time histories (in 3 dimensions). In this study linear time history analysis is preferred, as the design of the structural members based on load combinations in low-rise and mid-rise buildings is based on linear behavior assumptions. The simulations are performed in two separate settings. One, the structural models are analyzed under 2-D ground motions (Two Horizontal components); and is followed by 3-D (Two Horizontal components and One Vertical component) application of same ground motions.

CHAPTER 2

MODELS AND GROUND MOTIONS

2.1. Models` Details

This study considers four Steel Special Moment Resisting Frame (SMRF) and four Special Concentric Braced Frame (SCBF) structures, whose main design characteristics are provided in Appendix (Tables A1 and A2, respectively). The design for both types of structures is derived from NIST (2010). All the buildings are designed for Downtown, Los Angeles, CA with Site Class *D* conditions. The schematic illustration of the SMRF and SCBF structures is provided in Figure 2.1.

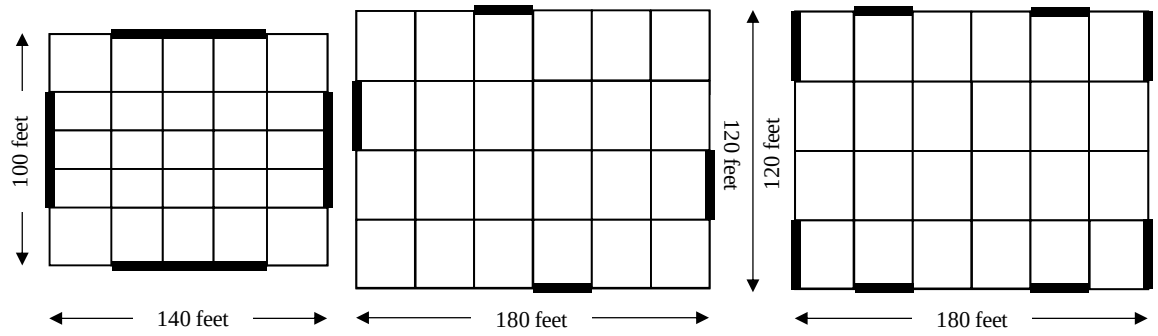

Figure 2.1– Building plan views: (a) all SMRFs, (b) 3-Story and 6-Story SCBF, (c) 12-Story and 16-Story SCBF. (Lateral load resisting frames are marked with heavy black lines)

SMRF buildings consist of 2-, 4-, 8- and 12-story structures. The member sizes for beams and columns of respective stories are given in Appendix 1 (Tables A3 to A6). Referring to Figure-2.1(a), SMRF buildings have frames on perimeter edges and all frames consist of 3 bays. While the 2-story building exhibits greater base flexibility and has a pinned base, all the other building (4-story, 8-story, and 12-story) are designed with a fixed base. SMRF buildings are designed with

a floor plan of dimensions 140 *feet* by 100 *feet*. The moment frames are designed to resist seismic design loads and the gravity loads of the tributary areas. Each building consists of frames with different member sizes, however, certain traits are common in all the buildings:

1) The bay width for all the frames is equal to 20 *feet*.
2) The height of the first story is 15 *feet* while other stories have a height of 13 *feet.*
3) All the moment frames connections (beam-to-column connections) are designed as Reduced Beam Section (RBS) connections.

SCBF buildings consist of 3-, 6-, 12- and 16-story structures. The member sizes for braces and columns of respective stories are provided in Appendix (Tables A7 to A10). All SCBF buildings are designed with a cross-bracing configuration that spans two stories. All the structures are provided with braced bays at the building perimeter. To produce lower bound designs without excessive overstrength, the number of braced bays were varied to optimize the strength as per level of seismic design loading. While the 3-story and 6-story buildings are provided with one braced bay at each edge, the 12-story and 16-story buildings are designed with two braced bays at each edge. Figure 2.1(b) and Figure 2.1(c) display the location of braced frames on the perimeter of the 3-story and 6-story buildings, and the 12-story and 16-story buildings, respectively. The 3-story SCBF building exhibits greater base flexibility and is designed with a pinned base, while all the other SCBF buildings are designed with a fixed base. The buildings are assumed to have no horizontal irregularities, no extreme torsional irregularities, and the braced frames in any one plane take less than 60% of the total seismic force in that direction. Each building consists of frames with different member sizes, however, certain traits are common in all the buildings:

1) The bay width for all the frames is equal to 30 *feet*.

2) All stories have a height of 15 *feet*.

In both types (SMRF and SCBF) of buildings, a uniform dead load of 100 *psf* is applied to all stories. The diaphragms of all floors distribute a reduced live load of 50 *psf* except the roof where a live load of 25 *psf* is applied. Cladding load of 25 *psf* is applied on the perimeter of each story.

2.2. Ground Motions

Two groups of near-field ground motions are used in this research. Group 1 includes ground motions generated by strike-slip faulting and group 2 includes ground motions from reverse fault mechanism. From previous research, it is deduced that near-fault (source to site distances less than 15 *km*) ground motions possess significant vertical components and hence have larger detrimental impact on the structures than the far-field ones (Bozorgnia *et al.*, 1995; Kunnath *et al*., 2008; Elnashai *et al*., 2014; Collier *et al*., 2001). Therefore, for each group, 30 sets of unscaled near-fault ground motions with magnitude above 6.5 are selected from NGA2WEST (Timothy *et al*. 2014) database. The details of strike-slip ground motions and reverse fault ground motions are provided in Appendix (Tables A11 and A12 respectively). These unscaled near-fault ground motions are used for linear time history analysis of the structures. *RotD50* at the first mode period of each building is used as the Intensity Measure (*IM*). *RotD50* is the median value of the spectral acceleration obtained when the 2 horizontal components are applied orthogonally and rotated throughout 180 degrees on a Single Degree of Freedom (SDOF) system with a varying spectral period (Bozorgnia *et al.*, 2016). The *RotD50* of the 60 ground motions used in this study are obtained from NGA2WEST database.

CHAPTER 3

METHODOLOGY

3.1. Methodology Steps

Reliability Index of the steel structural members is calculated and compared for four cases. The cases are classified based on how the *effective* nominal resistance (R_n) of the components is derived and whether the components are analyzed under 2-D ground motions (2 Horizontal components only) or 3-D ground motions (2 Horizontal and 1 Vertical component). The four cases of analysis are explained in Table-3.1.

Table 3.1: Analysis cases and ground motion configurations

Analysis Case	Effective Nominal Resistance (R_n)	Analyzed Under
Case I	$(1.2D_n + 0.5L_n + 1.0E_n)/0.9$	2-D Ground Motions
Case II	$(1.2D_n + 0.5L_n + 1.0E_n)/0.9$	3-D Ground Motions
Case III	$\left((1.2 + 0.2S_{DS})D_n + 0.5L_n + 1.0E_n\right)/0.9$	3-D Ground Motions
Case IV	2% Drift Based Design	3-D Ground Motions

The term e*ffective* in this study is defined as the value derived from the design criteria rather than the actual value which is based on subjective decisions. Hence, e*ffective* nominal resistance (R_n) is defined as the nominal resistance obtained directly from the design criteria rather than the actual member strength.

To obtain the Reliability Index (β), First Order Reliability Method (FORM) is conducted on the limit state equations for structural component actions. A detailed 6-step procedure to arrive at the limit state equations and to finally obtain β is explained below.

i. Step 1

By performing linear time history analysis of the structures under each ground motion, the Engineering Demand Parameters due to Earthquake Loading (*E*) of each member (beams, braces, columns) for respective component actions (moment and shear for beams, axial load and moments for columns, and axial load for braces) are captured. In this research, linear time history analysis is preferred, as the design of the structural members based on load combinations in low-rise and mid-rise buildings is usually grounded on linear behavior assumptions. On each story, the critical member of each member type (i.e., beams, braces, and columns) is defined as the member undergoing the largest seismic demand. This is distinctly done for all the component actions (i.e., moment, shear force, axial load). This means, for example, that in an SMRF structure, one value of moment (maximum value among all beam moments) and one value of shear force (maximum value among all beam shear forces) on each story is considered as the seismic demand value for beam moment and beam shear, respectively. Similarly, for columns in SMRF and SCBF buildings and braces in SCBF buildings, critical members on each story are identified and seismic demands are apprehended for their respective component actions. Depending on the type of building, the component actions analyzed for the corresponding type of member are given in Table 3.2.

Table 3.2: Classification of members and associated EDPs

Building Type	Member Type	Component Action	Location of member at which EDP is considered
SMRF	Beams	Moment	Right and Left End (at RBS)
		Shear Force	Right and Left End (at RBS)
	Columns	Axial Load	Top and Bottom
		Moment	Top and Bottom
SCBF	Braces	Axial Load	Top and Bottom
	Columns	Axial Load	Top and Bottom
		Moment	Top and Bottom

A power function as shown in Eq. (4) is used to correlate seismic demands to ground motion intensity measure (i.e., *RotD50* component of the ground motion at the building`s first mode period denoted as S_a) (Cornell *et al.* 2002). Since load demands depend on member type and corresponding component action (moment and shear for beams, axial load and moments for columns, and axial load for braces), for the sake of brevity, Engineering Demand Parameters (EDP) due Dead Load, Live Load and Earthquake Load are represented as *D*, *L* and *E*, respectively; the corresponding Resistance is denoted as *R*. In Eq. (4), $\hat{E}$ represents the median value of the EDP due to seismic loads, b = 1 (Luco *et al.*, 1998; Luco *et al.*, 2000), and a is derived by conducting regression analysis on $\left(LN(E), LN(S_a)\right)$ pairs. The seismic EDP values (E) are distributed lognormally with standard deviation of the natural logarithm of E, $\sigma_{LN(E)|S_a}$ (Shome *et al.*, 1999). The top right corner of block 3 of Figure 3.1 shows the process for generating such equations to correlate seismic demands and ground motion intensity measure.

$$\hat{E} = a(S_a)^b \tag{4}$$

ii. Step 2

Limit state equations are set up depending on the type of member and component action (denoted as $CA \in \{\text{Beam Moment}, \text{Beam Shear}, \text{Brace Axial Load}\}$). Four random variables are identified for reliability analysis; one for resistance and three for EDP values due to three types of loading (Dead Load, Live Load, and Earthquake Load). The distribution type of all four random variables (Ellingwood *et al.*, 1980) and corresponding equations for Cumulative Probability Distribution Function (CDF) and statistical parameters (Mean and Standard Deviation) of the distributions are provided in Table 3.3.

Table 3.3: Probability distribution functions associated with loads and resistance

R.V.	Dist.	CDF	Mean(μ)	Standard Deviation(σ)
Resistance	Lognormal	$\Phi\left(\frac{\ln(x)-\mu}{\sigma}\right)$	$\exp\left(\mu+\frac{\sigma^2}{2}\right)$	$\sqrt{(\exp(\sigma^2)-1)(\exp(2\mu+\sigma^2))}$
Dead Load	Normal	$\Phi\left(\frac{x-\mu}{\sigma}\right)$	μ	σ
Live Load	Gamma	$\frac{\lambda(\lambda x)^{k-1}exp(-\lambda x))}{\Gamma(k)}$	$\lambda\sigma^2$	$\frac{\mu}{\sqrt{k}}$
EQ Load	Type-II Extreme	$\exp\left[-\left(\frac{u}{x}\right)^k\right]$	$u\,\Gamma\left(1-\frac{1}{k}\right)$	$u\sqrt{\Gamma\left(1-\frac{2}{k}\right)-\Gamma^2\left(1-\frac{1}{k}\right)}$

For beams and braces, $Z_{CA} = R_{CA} - D_{CA} - L_{CA} - E_{CA}$ is used as the limit state equation, where *D*, *L*, *E* and *R* represent random variables for EDP due to Dead Load, EDP due to Live Load, EDP due to Earthquake Load and corresponding resistance, respectively. The subscript *CA* denotes the respective component action (e.g. D_{Axial} represent the random variable associated with Axial Load due to Deal Load). While for columns, due to the PM interaction, the limit state equation used is, $Z_{Col} = 1 - \frac{(D_{Axial}+L_{Axial}+E_{Axial})}{R_{Axial}} - \frac{(D_{Moment}+L_{Moment}+E_{Moment})}{R_{Moment}}$.

iii. Step 3

To conduct reliability analysis and calculate β, the type of distribution and statistical parameters (i.e. mean and standard deviation) of each random variable is estimated. This step involves conducting non-linear regression analysis and maximum likelihood estimation to derive the statistical parameters of the distribution function representing EDP due to Earthquake Load (*E*) (i.e. $P[E \geq e]$). Using total probability theorem, λ_E can be written in continuous integral form as shown in Eq. (5) (Cornell *et al.*, 2002). Using OpenSHA (or any other probabilistic hazard analysis software) with IM set as *RotD50* for the corresponding building period, the spectral acceleration hazard curve in the form of Probability of Exceedance ($G_{S_a}(s_a)$) is obtained. Using the Poisson`s

Model with Period of Interest (i.e. life span, denoted as *t*) as 50 years and the procured Probability of Exceedance ($G_{S_a}(s_a)$), Annual Rate of Exceedance (λ_{S_a}) is acquired using Eq. (6). Hazard levels in the proximity of limit state probability (S_a with average return period between 25 years to 2500 years) can be represented in the form Eq. (7) (Jalayer *et al.,* 2003). By fitting a power curve on the obtained spectral acceleration hazard, parameters k_0 and k are estimated. Upon integration, and simplification, Eq. (5) will convert to Eq. (8). Furthermore, Poisson`s model (Eq. (9)) is used to acquire $G_E(e)\ i.e. P[E \geq e]$, from λ_E. $G_E(e)$ is calculated for a wide range of values of e.

$$\lambda_E = \int P(E \geq e|S_a = s_a)|d\lambda(s_a)| \tag{5}$$

$$G_{S_a}(s_a) = P[S_a \geq s_a] = 1 - \exp\left(\lambda_{S_a} t\right) \tag{6}$$

$$\lambda_{S_a} = k_0 {S_a}^{-k} \tag{7}$$

$$\lambda_E = k_0 ({}^{e}/_{a})^{-k} exp\left[\frac{1}{2}\frac{k^2}{b^2}{\sigma_{LN(E)|S_a}}^2\right] \tag{8}$$

$$G_E(e) = P[E \geq e] = 1 - \exp(\lambda_E t) \tag{9}$$

Using $G_E(e)$, the Cumulative Distribution Function (i.e. $F_E(e)$) of Type-II Extreme Distribution can estimated by $F_E(e) = 1 - G_E(e)$. The parameters of this distribution are estimated by using maximum likelihood estimation and performing nonlinear regression on the response data. Although more accurate methods of approximating the hazard curve and performing closed form integral of Eq. (6) are available (Vamvatsikos 2012), for the sake of brevity, the authors have limited the computation to the method described above. This process is repeated for each member type for all component actions on each story, thereby, obtaining means and standard deviations of respective EDPs due to Earthquake Load for all critical members for the corresponding component action (E_{CA}).

iv. Step 4

This step involves estimation of statistical measures (mean and standard deviation) of EDP due to Dead Load (D) and EDP due to Live Load (L) for each component action. The distribution type and statistical measures of D and L are estimated by the 'Mean to Nominal' ratios and 'Coefficients of Variation' (V) provided in Table 3.4 (Ellingwood *et al.* 1980). Nominal EDP values due to Dead Load and Live Load on every critical member for all component actions are obtained by conducting dead load and live load analysis separately. The applied nominal Dead Load and Live Load values are explained in Section 2. Once the nominal value of EDP due to Dead Load (D_n) and the nominal value of EDP due to Live Load (L_n) are procured, using the data provided in Table 3.4, the distributions and the statistical measures of random variables for Dead Load and Live Load are obtained. This process is repeated for each member type for all component actions on each story, thereby, obtaining means and standard deviations of respective EDP values due to Dead Load and Live Load for all critical members for the corresponding component action i.e. D_{CA} and L_{CA}, respectively.

Table 3.4: Mean to Nominal ratios and Coefficient of Variation for Dead and Live loads

Random Variable	Dist.	$\frac{\text{Mean}}{\text{Nominal}}$	C.o.V. (V)
Dead Load	Normal	1.05	0.1
Live Load	Gamma	0.25	0.55

v. Step 5

After obtaining the statistical measures of each EDP, mean and standard deviation of resistance (R) is estimated. The resistance in this study does not refer to the actual (i.e. plastic strength) of the member but rather is the *effective* resistance derived from specific design criteria (see Table

3.1). The *effective* nominal resistance for three component actions of Moment for Beams, Shear for Beams, and Axial Load for Braces is derived from Eqs. (10) and (11) for Analysis Case I and II and Analysis Case III, respectively. γ_D = 1.2 is the partial safety Factor for Dead Load, γ_L = 0.5 is the partial safety factor for Live Load (arbitrary point load), ρ = 1.0 is the Redundancy Factor, ϕ= 0.9 is the partial safety factor of resistance, S_{DS} = 1.0g is the short period design spectral acceleration obtained from USGS design maps for site class *D*. For each component action (denoted as *CA*), D_n and L_n are the nominal EDPs due to Dead Load and Live Load calculated from dead load and live load analysis, respectively and E_n is the nominal EDP due to Earthquake Load obtained from response spectrum analysis with design spectrum parameters S_{DS} = 1.0 g and S_{D1} = 0.6 g.

$$R_{n,CA} = \frac{\gamma_D D_{n,CA} + \gamma_L L_{n,CA} + \rho E_{n,CA}}{\phi} \quad (10)$$

$$R_{n,CA} = \frac{(\gamma_D + 0.2 S_{DS}) D_{n,CA} + \gamma_L L_{n,CA} + \rho E_{n,CA}}{\phi} \quad (11)$$

Analyses show that columns are controlled by limit state of plastic moment, hence, possess an axial and moment strength equal to $R_y F_y A_g$ and $R_y F_y Z_x$, respectively, where R_y = 1.1 is the ratio between actual and expected yield strength, F_y = 50 ksi is the expected yield strength, and A_g and Z_x are the gross area and plastic section modulus of the provided steel sections, respectively. However, similar to the case of beams and braces, the *effective* nominal resistance for each component action ($R_{n,CA}$) is derived from the design criteria. For all column sections (W12, W14 etc.), it is noticed that the plastic section modulus (Z_x) and gross area (A_g) follow a linear relation: $Z_x = mA_g + n$. By performing a linear regression, coefficients *m* and *n* are estimated for each column section separately. Then *effective* gross area (A_{ge}) is estimated for each critical column using Eq. (12) and Eq. (13) for Analysis Case I and II and Analysis Case III, respectively. Using

estimated value of A_{ge}, *effective* plastic modulus ($Z_{xe} = mA_{ge} + n$) for the column section is calculated. The *effective* nominal resistance of axial load ($R_{n,Axial}$) and *effective* nominal resistance of moment of columns ($R_{n,Moment}$) are then calculated shown in Eqs. 14 and 15.

$$\frac{\gamma_D D_{n,Axial} + \gamma_L E_{n,Axial} + \gamma_E E_{n,Axial}}{\phi R_y F_y A_{ge}} + \frac{\gamma_D D_{n,Moment} + \gamma_L L_{n,Moment} + \gamma_E E_{n,Moment}}{\phi R_y F_y (mA_{ge} + n)} \leq 1 \qquad (12)$$

$$\frac{(\gamma_D + 0.2S_{DS}) D_{n,Axial} + \gamma_L E_{n,Axial} + \gamma_E E_{n,Axial}}{\phi R_y F_y A_{ge}} + \frac{(\gamma_D + 0.2S_{DS}) D_{n,Moment} + \gamma_L L_{n,Moment} + \gamma_E E_{n,Moment}}{\phi R_y F_y (mA_{ge} + n)} \ldots . \leq 1 \qquad (13)$$

$$R_{n,Axial} = \phi R_y F_y A_{ge} \qquad (14)$$

$$R_{n,Moment} = \phi R_y F_y Z_{xe} \qquad (15)$$

According to ASCE 7, inelastic drifts at each story of SMRFs are limited to 2%. Hence, structural members should be sized to attain a drift of 2% or less, which results in a member size greater than what is required by the load combinations. In this study, the elastic story displacements (Δ) for all stories are derived using pushover analysis using the ASCE 7 suggested load pattern and base shear coefficient. To limit story drifts to 2%, the provided members` strengths are adjusted by using a factor *phi* ($\boldsymbol{\Phi} = \frac{\Delta}{\Delta_{limit}}$). Factor $\boldsymbol{\Phi}$ is used to calculate the required gross area ($A_{g_{Reqd}}$), required plastic modulus ($Z_{x_{Reqd}}$) and required shear web area ($A_{w_{Reqd}}$) of beams and columns, which signify the minimum geometrical properties of members required to limit the drifts exactly to 2%. Using $\boldsymbol{\Phi}$, the $A_{g,Reqd}$, $Z_{x,Reqd}$ and $A_{w,Reqd}$ is calculated as shown in Eqs. (16) , (17) and (18) where A_g, Z_x and A_w being the actual gross area, plastic modulus, and web area of the provided steel *W* sections.

$$A_{g_{Reqd}} = \boldsymbol{\Phi} A_g \qquad (16)$$

$$Z_{x_{Reqd}} = \boldsymbol{\Phi} Z_x \qquad (17)$$

$$A_{w_{Reqd}} = \mathbf{\Phi} A_w \quad (18)$$

Then, for Analysis Case IV, the *effective* nominal moment resistance ($R_{n,Moment}$) and *effective* nominal shear resistance ($R_{n,Shear}$) in beams and *effective* nominal axial load resistance ($R_{n,Axial}$) and *effective* nominal moment resistance ($R_{n,Moment}$) in columns is calculated as shown in Eqs. (19) - (21).

$$R_{n,Moment} = \phi R_y F_y Z_{x_{Reqd}} \quad (19)$$

$$R_{n,Shear} = 0.6 R_y F_y C_v A_{w_{Reqd}} \quad (20)$$

$$R_{n,Axial} = \phi R_y F_y A_{g_{Reqd}} \quad (21)$$

As per Ellingwood *et al*. (1980), the mean value of random variable of resistance for any component action (R_{CA}) is equal to 1.18 times the nominal value of resistance of the corresponding component action ($R_{n,CA}$) and the coefficient of variation of random variable of resistance (V_R) is equal to 0.13. By these ratios and already calculated nominal values for resistance at each story, the mean value and standard deviation of the random variable of resistance for each component action (R_{CA}) for every critical member are calculated in all four analysis cases. Thus, the distributions and statistical parameters of all four random variables are recognized. This leads to the final step of calculation of Reliability Index (β).

vi. Step 6

In the final step, the derived statistical parameters for each Random Variable (Resistance, Dead Load, Live Load and Earthquake Load) are used to calculate Reliability Index (β) by conducting a First Order Reliability (FORM) Analysis. First Order Reliability Method (FORM) is used to

calculate Reliability Index (β). As discussed before, FORM analysis involves selection of *MPP* or design point at the failure surface (where $Z = 0$). This procedure is explained in generalized terms as follows. Suppose the limit state function relating the resistance and load variables is given by Eq. 22

$$g(X_1, X_2, X_3, \ldots., X_n) = 0 \tag{22}$$

X_i represents basic random variable for resistance or load and failure occurs when $g < 0$ for any limit state. The random variables X_i are first transformed into reduced coordinate variables having mean of zero and variance of unity using Eq. 23

$$x_i = \frac{X_i - \mu_{X_i}}{\sigma_{X_i}} \tag{23}$$

$\mu_{X_i}$and σ_{X_i} are the mean and standard deviation of random variable X_i. The limit state in the reduced coordinate system is expressed as Eq. 24

$$g(x_1, x_2, x_3, \ldots., x_n) = 0 \tag{24}$$

x_i = reduced resistance or load random variable and failure occurs when $g < 0$ for any limit state. As stated earlier, reliability index (β) is the shortest distance between the failure surface ($Z = 0$, in this example: $G = 0$ or in reduced system $g = 0$) and the origin. The corresponding point where $g = 0$ is known as most probable point (*MPP*) or the design point and is designated as u_i^*.

If the basic random variables have non-normal distribution, an approximate equivalent normal distribution at the design point having same tail area and ordinate of the density function is

designated with equivalent mean ($\mu_X{}^N$) and equivalent standard deviation ($\sigma_X{}^N$) as expressed in Eqs. 25 and 26

$$\mu_X{}^N = u_i{}^* - \Phi^{-1}\left[F_{X_i}(u_i{}^*)\right]\sigma_X{}^N \tag{25}$$

$$\sigma_X{}^N = \frac{\phi\left\{\Phi^{-1}\left[F_{X_i}(u_i{}^*)\right]\right\}}{f_{X_i}(u_i{}^*)} \tag{26}$$

$F_{X_i}(u_i{}^*)$ is the original Cumulative Distribution Function (*CDF*) of X_i evaluated at design point, $f_{X_i}(u_i{}^*)$ is the original Probability Density Function (*PDF*) of X_i evaluated at design point, Φ[ ] is the *CDF* of standard normal distribution and ϕ [ ] is the *PDF* of the standard normal distribution.

The design point $u_i{}^*$ is obtained by solving a system of equations and searching for directions cosines ($\alpha_i{}^*$) that minimizes β.

$$\alpha_i{}^* = \frac{\left(\partial g/\partial x_i\right)\sigma_X{}^N}{\sqrt{\sum_{i=1}^{n}\left(\partial g/\partial x_i\right)^2}} \qquad \text{for } i = 1, 2, 3, \ldots\ldots, n \tag{27}$$

$$u_i{}^* = -\beta\,\alpha_i{}^* \tag{28}$$

$$g(u_1{}^*, u_2{}^*, u_3{}^*, \ldots\ldots, u_n{}^*) = 0 \tag{29}$$

The process is repeated until value of β converges. The value of β then obtained is the shortest distance from origin to failure surface in reduced coordinate system. In basic coordinate system, the design point or *MPP* is given by Eq. 30

$$U_i{}^* = \mu_{X_i} - \alpha_i{}^*\sigma_{X_i}\beta \tag{30}$$

$$g(U_1^*, U_2^*, U_3^*, \ldots\ldots, U_n^*) = 0 \quad (31)$$

The explained methodology is incorporated in this study for both types of buildings to arrive at the Reliability Index (β) of each critical member for each component action on every story as explained in *Step 2*. This is summarized in the pictorial flowchart provided in Figure 3.1, with step numbers provided at the top left corner of each block.

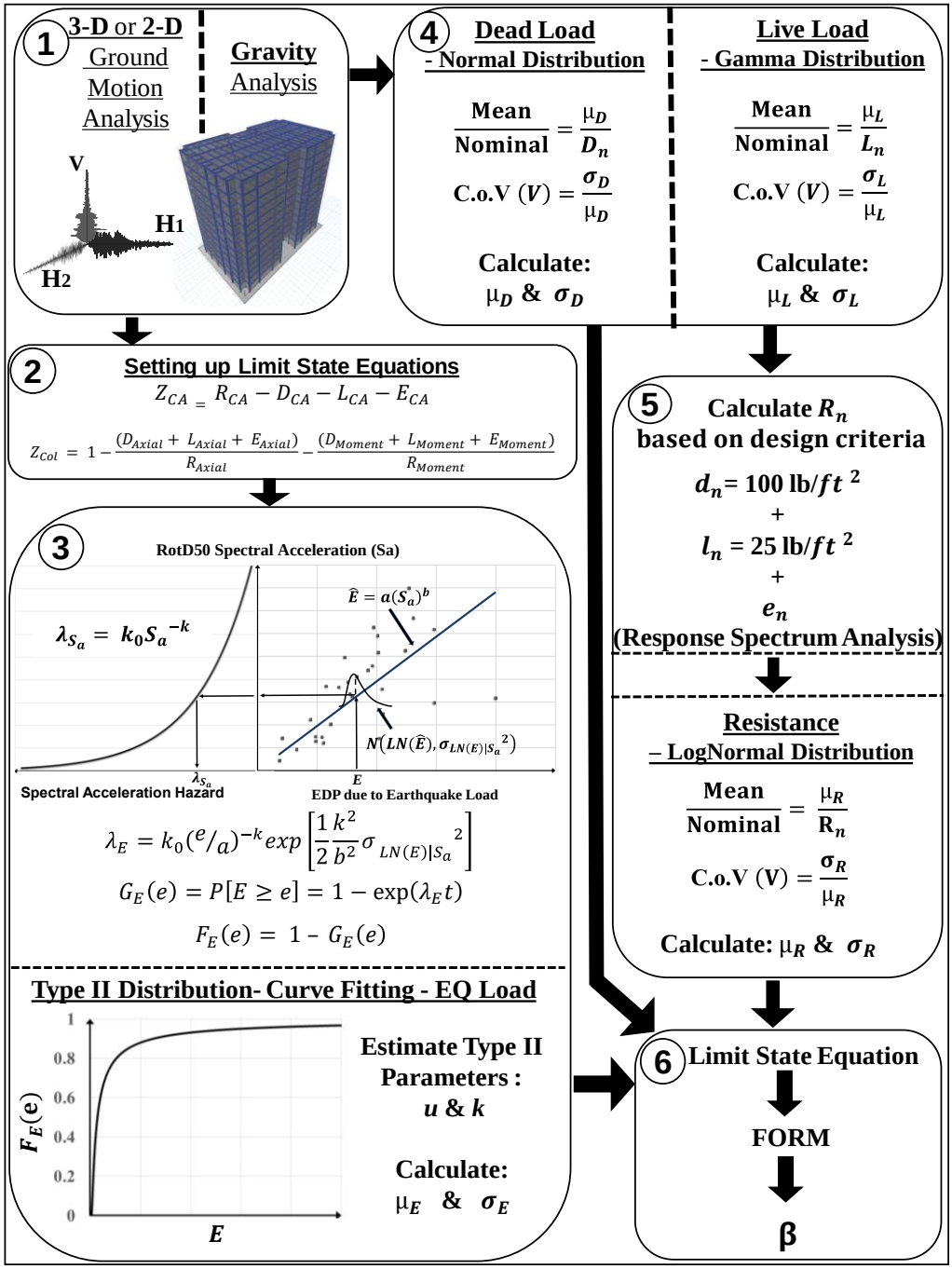

Figure 3.1– Methodology Flow Chart

CHAPTER 4

RESULTS AND DISCUSSION

The list of random variables along with their respective distribution type and statistical measures are provided in Table 4.1. Results show that the *k* parameter of Type-II Extreme CDF representing EDPs due to Earthquake Load (*E*) varies from 2.01 to 2.33 depending on the site hazard and consistently averages at a value of 2.17. This is in contrast with k = 2.3 used previously by Ellingwood *et al.* (1981). The reliability indices for SMRF and SCBF buildings are provided in terms of box and whisker diagrams in Figure 4.1-4.6, where minimum, first quartile, median, third quartile and maximum values of β are displayed.

Table 4.1: Properties of loads and resistance random variables

Random Variable	**Dist.**	**$\frac{\text{Mean}}{\text{Nominal}}$**	**C.o.V. (V)**	**$\frac{\text{Nominal R.V.}}{\text{Nominal Dead Load}}$**
Resistance	Lognormal	1.18	0.13	5 to 15
Dead Load	Normal	1.05	0.1	1
Live Load	Gamma	0.25	0.55	0.25
EQ Load	Type-II Extreme	0.5 to 0.9	1.5 to 3	5 to 10

4.1. Special Moment Resisting Frame (SMRF) Buildings

The results of reliability indices β calculated from the four analysis cases are presented in Figure 4.1(a) and Figure 4.1 (b) for beams and columns respectively. SMRF beams used in this study have long spans and are controlled by flexure. Hence, the values of β for moments in beams is less than

β values for shear, indicating that the beams experience a higher load/capacity ratio in terms of moments as compared to that of shear. It is observed that when the members are designed based on older seismic design load combination ($1.2D_n + 0.5L_n + 1.0E_n$) and the vertical component of ground motions is excluded from the analysis (Case I), the value of β for beams averages around 1.55 (probability of failure = 6%) near to the target reliability index of 1.75 while the reliability of columns seems to meet the target reliability requirements and β averages around 1.7. However, by including the vertical component of ground motion in the analysis (Case II) of members designed based on older seismic design load combination ($1.2D_n + 0.5L_n + 1.0E_n$), on average depreciates β of beams by 0.25 (to β = 1.35) and columns by 0.3 (to β = 1.4), increasing probability of failure to 8.8% and 8.2%, respectively. The vertical component of strong near-fault ground motions causes vigorous motions in floor slabs which leads to amplified axial force demands in the columns, and moment demands in the beams, thereby resulting in relatively lower reliability of both beams and columns. It is further inferred that by increasing the capacity of the members by current code provision of $0.2S_{DS}$ times Dead Load and using design load combination $(1.2 + 0.2S_{DS})D_n + 0.5L_n + 1.0E_n$ to account for the effect of vertical component of ground motions (Case III) only increases the reliability indices β by 0.1 on average, leading to β of 1.45 and 1.5 for beams and columns, respectively. β of 1.45 and 1.5 signifies probability of failure equivalent to 7.35 % and 6.68%, respectively, which is higher than the intended probability of failure of 4%. Thus, it appears that the factor of $0.2S_{DS}$ is incapable of entirely capturing the effects of the vertical component of ground motions.

SMRF structural design, however, is usually based on drift criteria rather the load criteria. The reliability of SMRF members based on the drift criteria is presented alongside in the Figures 4.1, 4.2

and 4.3. As expected, β of the members designed on basis of the drift criteria (Case IV) is much higher than β values for designs based on seismic load combination. β values of beams and columns designed on the basis of drift limit criteria averages above the value of 2, which is well higher than the target reliability β_T of 1.75.

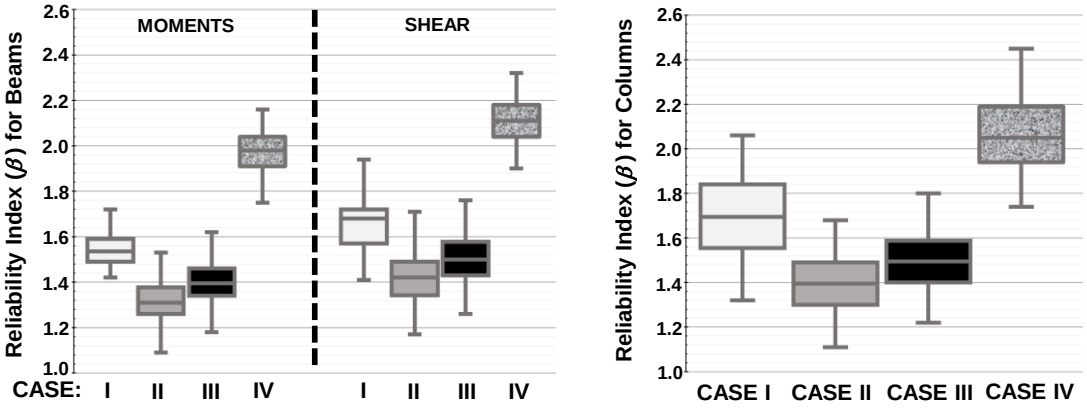

(a) (b)

Figure 4.1: Reliability index for SMRF members: (a) beams due to moment and shear, (b)columns due to axial load and moment (PM Interaction)

It is observed that the effect of the vertical component of ground motions from earthquakes generated by reverse faulting is large compared to the motions arising from strike-slip faulting. Compared to average β calculated in case of excluding vertical component of ground motions, the average drop in β due to the vertical component of reverse-fault ground motions is 0.28 and 0.36 for beams and columns, respectively, while the drop in β due to the vertical component of strike-slip ground motions is 0.21 and 0.25 for beams and columns. The results of the four design criteria bifurcated on the type of faulting are provided in Figure 4.2 and Figure 4.3. As the β of structural members designed without the inclusion of vertical component is similar under both groups of ground motions, it is exhibited that the ground motions originating due to reverse fault mechanism possess a larger vertical component which is the primary reason for the higher drop in value of β.

The reliability of individual members in SMRFs was further analyzed based on their location in the frame. The exterior ends of external beams tend to be the most critical among other locations. β of exterior end of external beams, on average, was 7.8% lower than the β of external beam's internal end, and 5.1% lower than the average β of internal beams. Similarly, on average, 3.4% lower values of β were observed for internal columns as compared to the external columns for both top and bottom ends, thereby indicating internal columns are more critical than the external ones irrespective of the inclusion of vertical component of ground motions in analysis. The bottom end of columns, on average, had a 3.1% lower β.

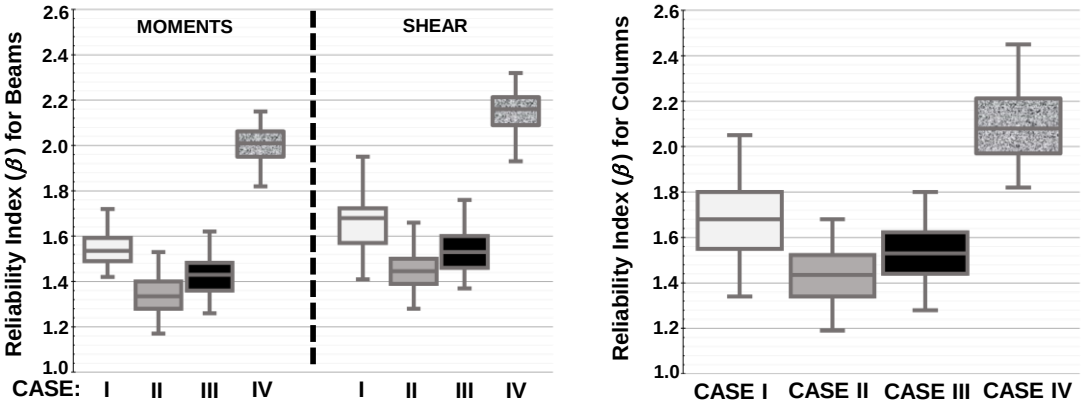

(a) (b)

Figure 4.2: Reliability index for SMRF members considering strike slip ground motions: (a) beams due to moment and shear, (b) columns due to axial load and moment (PM Interaction).

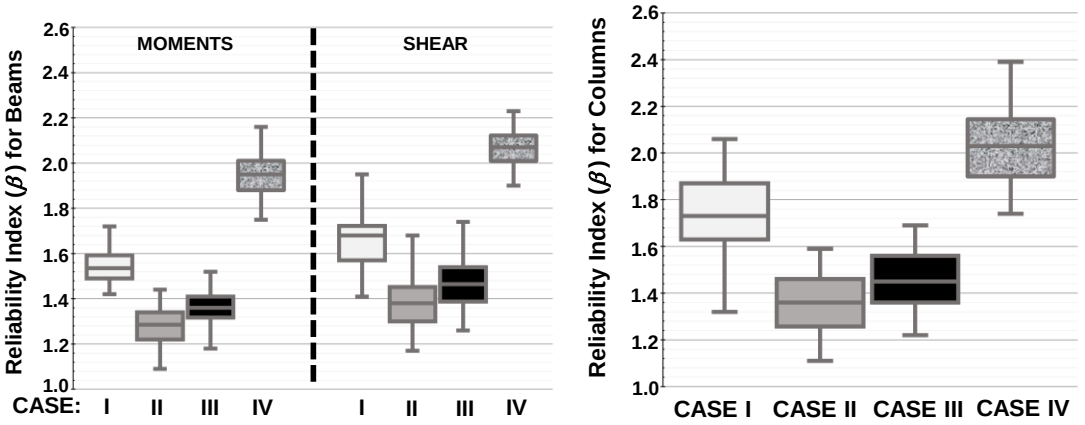

(a) (b)

Figure 4.3: Reliability index for SMRF members considering reverse fault ground motions: (a) beams due to moment and shear, (b) columns due to axial load and moment (PM Interaction).

4.2. Special Concentric Braced Frame (SCBF) Buildings

β values for the braces and columns based on three analysis criteria are given in Figure 4.4(a) and Figure 4.4(b), respectively. The value of β for both braces and columns designed without the incorporation of vertical component of ground motions as per the older seismic design load combination ($1.2D_n + 0.5L_n + 1.0E_n$) and analyzed under 2-D ground motions (Case I), averages at a value of 1.65 (probability of failure = 4.95%) which is close to the intended target reliability index of 1.75. Similar to SMRF structures, the inclusion of vertical component in the analysis of older seismic design load combination ($1.2D_n + 0.5L_n + 1.0E_n$) (Case II) decreases the reliability of both braces and columns. The vertical component of strong near-fault ground motions induces high vertical motion in the floor slabs which amplifies axial and moment demands. However, due to a good amalgamation of braces and columns, as vertical members, the drop in β in braces and columns is not observed to be as significant as that of SMRF members. Due to inclusion of vertical component in the analysis (Case II), an average drop of 0.24 in β (to β = 1.41, corresponding to probability of failure = 7.93%) is noticed in both braces and columns. Analysis of the buildings after incorporating ASCE 7 vertical component factor of $0.2S_{DS}$ in the member design load combination ($(1.2 + 0.2S_{DS})D_n + 0.5L_n + 1.0E_n$) to increase the capacity of the members (Case III), on average, increases the reliability indices of braces and columns by 0.11, thereby leading to β = 1.52 (probability of failure = 6.42%). This again supports the criticism against the incapability of ASCE 7 seismic load combination to accurately capture the effects of vertical component of ground motions. Irrespective of the design criteria, it is observed that the values of β for braces and columns are close.

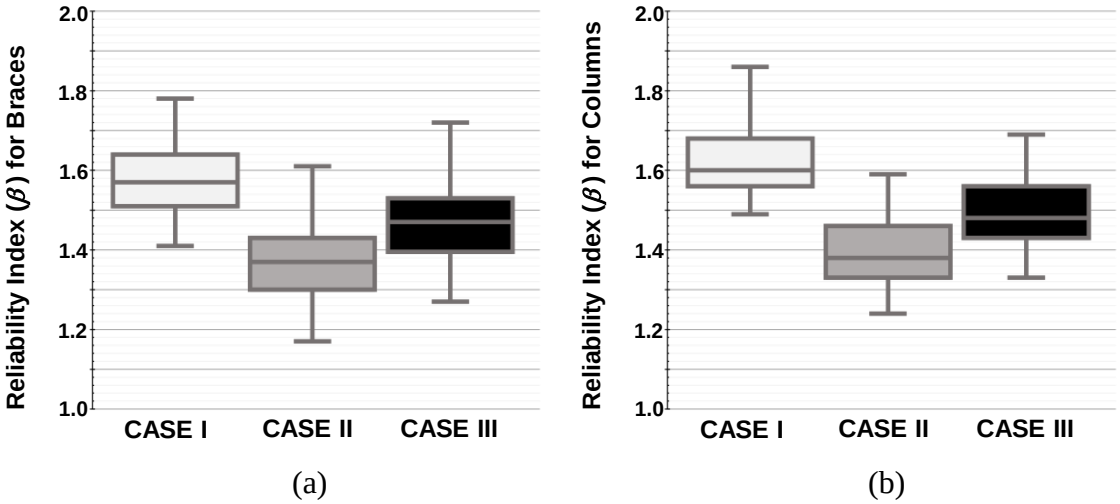

(a) (b)

Figure 4.4: Reliability index for SCBF members: (a) braces due to axial load, (b) columns due to axial load and moment (PM Interaction).

It is noticed that the drop in the reliabilities of SCBF members due to the incorporation of the vertical component is higher in the case of ground motions originating from reverse faulting as compared to strike-slip faults. In reverse fault ground motions, the average drop in β due to inclusion of the vertical component is around 0.28 while in strike slip the average drop in β is 0.21. This bolsters the fact that ground motions originating due to reverse fault mechanism possess a larger vertical component and results in larger decrease in the reliability of members. The results of the three design criteria, based on the type of faulting are provided in Figure 4.5 and Figure 4.6.

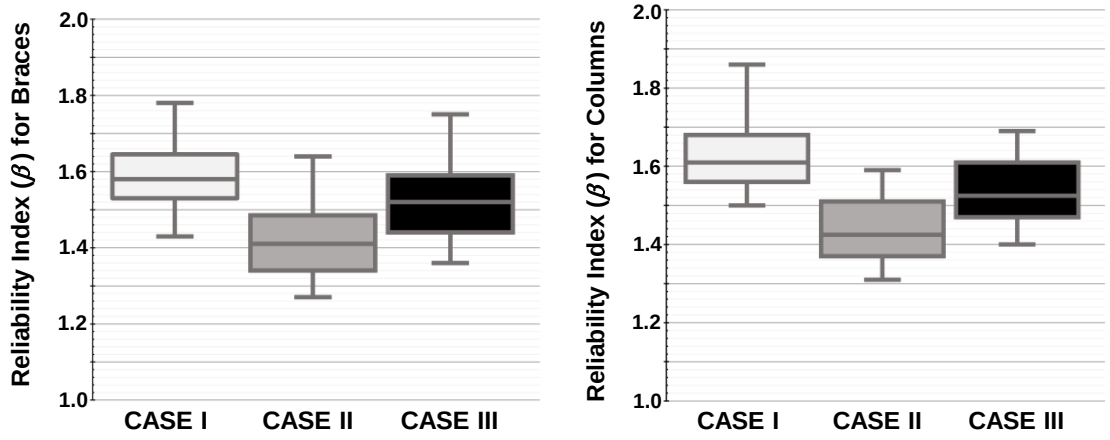

(a) (b)

Figure 4.5: Reliability index for SCBF members considering strike slip ground motions: (a) braces due to axial load, (b) columns due to axial load and moment (PM Interaction).

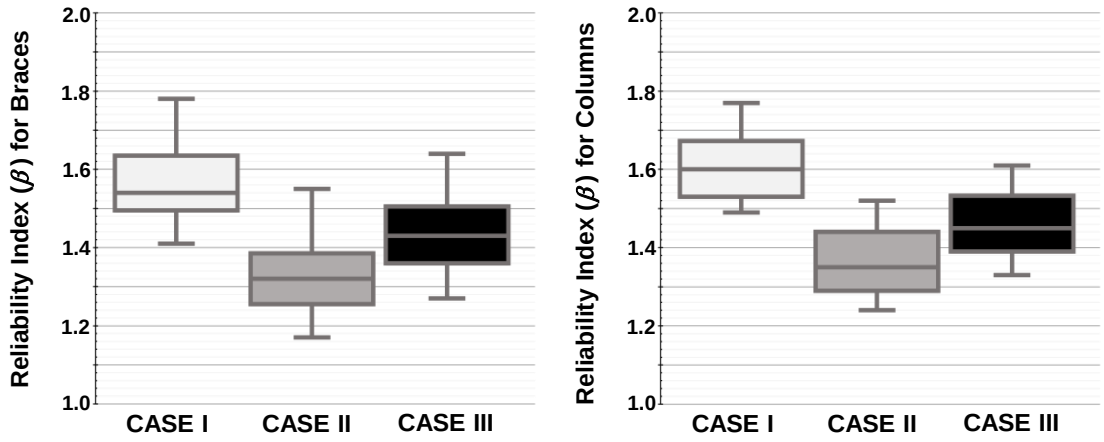

(a) (b)

Figure 4.6: Reliability index for SCBF members considering reverse fault ground motions: (a) braces due to axial load, (b) columns due to axial load and moment (PM Interaction).

4.3. Factors to Achieve Target Reliability (β_T)

As it is established that the current seismic load provision of using $0.2S_{DS}$ load factor on Dead Load to account for the effects of the vertical component is not an adequate practice, this study suggests an increase in the load factor to achieve the target reliability β_T = 1.75. Previous studies have criticized the use of this approach and the authors share that criticism. In lieu of any readily available solution, however, new empirical values for the load factor to attain the target reliability β_T = 1.75 are suggested. The lowest reliability index values in Analysis Case III (i.e. current seismic provision) are observed for the members undergoing 3-D ground motions arising from reverse faulting mechanism. Hence the reliabilities associated with these members are made a benchmark to calibrate new multiplier for S_{DS} as a load factor on Dead Loads (i.e. replacing the 0.2 value). This is done by using Eq. (32) for beam moments and brace axial loads and Eq. (33) for column PM interaction. In these equations, the value of x is back calculated by an iterative process so as to achieve a target reliability β_T = 1.75. This is distinctly done for beam moments, brace axial forces, and column PM

interaction for Case III type of analysis and ground motions originating from reverse faulting. The results of *x* values for minimum, first quartile, median, third quartile and maximum β of the above-mentioned members are provided in Tables 4.2, 4.3 and 4.4.

$$R_{n,CA} = \frac{(\gamma_D+(0.2+x)S_{DS})D_{n,CA} + \gamma_L L_{n,CA} + \rho E_{n,CA}}{\phi} \quad (32)$$

$$\frac{(\gamma_D+(0.2+x)S_{DS})D_{n,Axial} + \gamma_L E_{n,Axial} + \gamma_E E_{n,Axial}}{\phi R_y F_y A_{ge}} +$$

$$\ldots \frac{(\gamma_D+(0.2+x)S_{DS})D_{n,Moment} + \gamma_L L_{n,Moment} + \gamma_E E_{n,Moment}}{\phi R_y F_y (mA_{ge}+ n)} \leq 1 \quad (33)$$

Table 4.2: Multiplier to S_{DS} (i.e. (0.2+*x*)) to achieve $\boldsymbol{\beta_T = 1.75}$ (Case III, beam moments)

	Current Reliability	**Difference from $\boldsymbol{\beta_T = 1.75}$**	***x* value**
Minimum	1.18	0.66	3.56
First Quartile (25%)	1.32	0.53	2.29
Median (50%)	1.36	0.46	1.83
Third Quartile (75%)	1.41	0.41	1.4
Maximum	1.55	0.31	0.73

Table 4.3: Multiplier to S_{DS} (i.e. (0.2+*x*)) to achieve $\boldsymbol{\beta_T = 1.75}$ (Case III, brace axial force)

	Current Reliability	**Difference from $\boldsymbol{\beta_T = 1.75}$**	***x* value**
Minimum	1.27	0.48	2.39
First Quartile (25%)	1.36	0.39	1.76
Median (50%)	1.43	0.32	1.17
Third Quartile (75%)	1.50	0.25	0.64
Maximum	1.64	0.11	0.29

Table 4.4: Multiplier to S_{DS} (i.e. (0.2+x)) to achieve $\boldsymbol{\beta_T = 1.75}$ (Case III, column PM interaction)

	Current Reliability	**Difference from $\boldsymbol{\beta_T = 1.75}$**	***x* value**
Minimum	1.22	0.53	3.36
First Quartile (25%)	1.38	0.37	1.67
Median (50%)	1.45	0.3	1.12
Third Quartile (75%)	1.54	0.21	0.71
Maximum	1.69	0.06	0.19

Statistical representation of x for the combination of all component actions and types of ground motions can be used as a guide to suggest a single value of x which can be incorporated in seismic load combinations to satisfy $\beta_T = 1.75$. This is in contrast with the benchmark values of x presented in Tables 4.2, 4.3, and 4.4, where x values for specific component actions due to ground motions from reverse faulting mechanism are presented. The Probability Mass Function (PMF), and its equivalent Cumulative Density Function (CDF), of x for the combination of all component actions and types of ground motions is provided in Figure 4.7. For example, to assure 75% of members achieve $\beta_T = 1.75$, Figure 4.7 can be used to arrive at a $x = 1.45$.

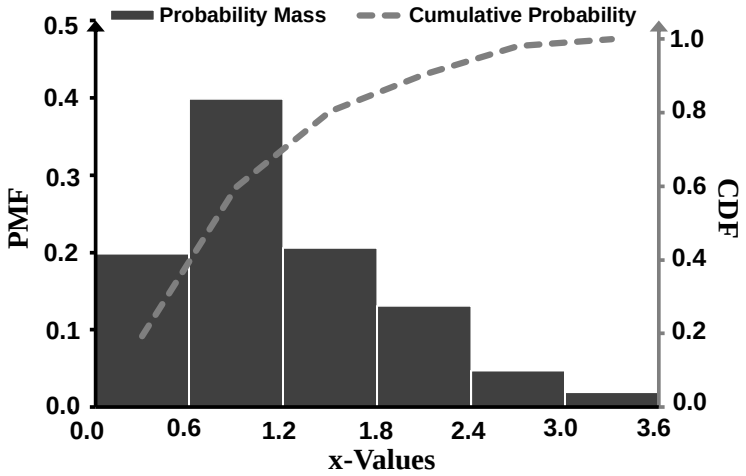

Figure 4.7: Probability Mass Function (PMF) and Cumulative Density Function (CDF) for proposed x values

CHAPTER 5

CONCLUSIONS

5.1. Summary and Conclusions

In the light of the recent research, the vertical component of ground motions continues to drive a debate on its effects and importance in the field of structural and earthquake engineering. Previous studies have investigated the effects of the vertical component of ground motions on engineered structures, however, a study that addresses the reliability of such structures considering this type of loading is absent. Meanwhile, previous research hypothesizes that the ASCE 7 approach for addressing the effect of vertical component of ground motions in the design of building structures is inadequate. This research shows that the suggested hypothesis is true.

The ASCE 7 code developers designed the seismic load combinations to achieve a target reliability index of 1.75 (probability of failure within 50-year lifetime = 4%). In this study, a total of eight low-rise and mid-rise steel buildings (four SMRF buildings and four SCBF buildings) are analyzed using a total of 60 sets of near-fault ground motions (30 sets of strike-slip ground motions and 30 sets of reverse fault ground motions). The effect of the vertical component of ground motions is evaluated based on the change in reliability index of the members of the earthquake-resistant system when vertical component of ground motions is incorporated in the design and assessment versus when only two horizontal components are considered. As mentioned in Table 3.1, this evaluation is conducted under 4 cases of analysis, which incorporate the designs based on basic code (ANSI A58 8.1-1980), current code (ASCE 7) and the 2% drift criteria.

The results of this research show that the reliability index for both SMRF and SCBF structural members obtained from the old seismic design load combinations ($1.2D_n + 1.0E_n + 0.5L_n$) (i.e., without the $0.2S_{DS}$ term in the Dead Load multiplier), if assessed under 2-D ground motions have reliability indices close to 1.75 (with probability of failure of 4%). However, inclusion of the vertical component of ground motions in seismic demand assessment increases the central value and variability of seismic demands and leads to lower reliability. With the incorporation of vertical component in the analysis of SMRF buildings, a decrease of 0.25 and 0.3 in value of β and hence an increase of 3.3% and 3.8% in probability of failure of beams and columns, respectively, is noticed. While in the case of SCBF members, including vertical component of ground motions in analysis decreases β by 0.24 increasing probability of failure of both braces and columns by 2.9%. Although in some structural members, due to the counteracting effect of the vertical component of ground motions, an increase in β was observed but for majority of cases significant decrease in reliability of members is noticed when the vertical component of ground motions is included in the analysis of buildings. This reflects that the vertical ground motions can substantially alter the seismic response of a structure and design based on the current ASCE 7 guidelines in which the effect of the vertical component of ground motions are represented by magnifying the dead loads by a factor equal to $0.2S_{DS}$ do not lead to satisfactory reliability indices for SMRF and SCBF members. Result of this study also show that factors as large as $(1.2 + 1.65)S_{DS}$ are required to be incorporated in the current seismic load combinations instead of $(1.2 + 0.2)S_{DS}$ in order to reach $\beta_T = 1.75$.

Furthermore, from this analysis, it can be deduced that the ground motions arising from reverse fault mechanism possess a higher vertical component resulting in 35% greater drop in reliability

of members as compared to those from the strike-slip mechanism. It is evident from the analyses presented in this study that the vertical component of ground motions is highly underestimated by the current seismic code design standards and more authenticated factors must be calibrated to appropriately account for the effects due to the vertical component of ground motions.

APPENDIX

A.1 Summary of Buildings

Table A1.1: Design Characteristics of Special Moment Resisting Frame Structures

Design Code	Number of Stories	R	$V_{RSA-Design}/W$	T_{code} (sec)	T_{1H} (sec)
ASCE 7-10	2	8	0.101	0.56	0.97
ASCE 7-10	4	8	0.074	0.95	2.01
ASCE 7-10	8	8	0.043	1.64	2.66
ASCE 7-10	12	8	0.030	2.25	3.8

*$V_{RSA-Design}$ is the Design Base Shear as determined from Response Spectrum Analysis using ASCE 7-10. It is assumed $R = C_d$.

*T_{code} is the natural period of the structure, as determined by ASCE 7-10.

*T_{1H} is the period of the first mode of vibration of the structure, as determined from eigenvalue analysis.

Table A1.2: Design Characteristics of Special Concentric Braced Frame Structures

Designing Council	Number of Stories	R	$V_{RSA-Design}/W$	T_{code} (sec)	T_{1H} (sec)
ASCE 7-10	3	6	0.153	0.49	0.61
ASCE 7-10	6	6	0.105	0.78	1.1
ASCE 7-10	12	6	0.058	1.3	1.99
ASCE 7-10	16	6	0.051	1.69	3.17

*$V_{RSA-Design}$ is the Design Base Shear as determined from Response Spectrum Analysis using ASCE 7-10. It is assumed $R = C_d$.

*T_{code} is the natural period of the structure as determined by ASCE 7-10.

*T_{1H} is the period of the first mode of vibration of the structure, as determined from eigenvalue analysis.

Table A1.3: Member Sizes for 2-story SCBF building

Story	Beams	External	Internal
2	W16x31	W24x131	W21x162
1	W30x132	W24x131	W21x162

Table A1.4: Member Sizes for 4-story SCBF building

Story	Beams	External	Internal
4	W21x57	W24x62	W24x62
3	W21x57	W24x62	W24x62
2	W21x73	W24x103	W24x103
1	W21x73	W24x103	W24x103

Table A1.5: Member Sizes for 8-story SCBF building

Story	Beams	External	Internal
8	W21x68	W24x94	W24x94
7	W24x84	W24x94	W24x94
6	W27x94	W24x131	W24x131
5	W27x94	W24x131	W24x131
4	W27x94	W24x131	W24x162
3	W30x116	W24x131	W24x162
2	W30x116	W24x131	W24x162
1	W30x108	W24x131	W24x162

Table A1.6: Member Sizes for 12-story SCBF building

Story	Beams	External	Internal
12	W24x84	W24x84	W24x94
11	W24x84	W24x84	W24x94
10	W27x94	W24x131	W24x131
9	W27x94	W24x131	W24x131
8	W30x116	W24x131	W24x162
7	W30x116	W24x131	W24x162
6	W30x116	W24x146	W24x176
5	W30x116	W24x146	W24x176
4	W30x132	W24x162	W24x207
3	W30x132	W24x162	W24x207
2	W30x132	W24x207	W24x207
1	W30x124	W24x207	W24x207

Table A1.7: Member Sizes for 3-story SCBF building

Story	Columns	Braces	Beams
3	W12x120	HSS8-3/4x0.312	W30x173
2	W12x120	HSS8-3/4x0.5	W21x111
1	W12x120	HSS9-5/8x0.5	W18x65

Table A1.8: Member Sizes for 6-story SCBF building

Story	Columns	Braces	Beams
6	W14x68	HSS7-1/2x0.312	W18x97
5	W14x68	HSS9-5/8x0.375	W24x104
4	W14x176	HSS9-5/8x0.5	W24x131
3	W14x176	HSS11-1/4x0.5	W18x76
2	W14x342	HSS12-1/2x0.5	W24x146
1	W14x342	HSS12-1/2x0.5	W21x62

Table A1.9: Member Sizes for 12 story SCBF building

Story	Columns	Braces	Beams
12	W12x45	HSS6-5/8x0.312	W18x55
11	W12x45	HSS6-5/8x0.312	W18x35
10	W14x99	HSS8-3/4x0.312	W18x60
9	W14x99	HSS8-3/4x0.312	W18x35
8	W14x193	HSS10x0.375	W18x65
7	W14x196	HSS10x0.375	W18x35
6	W14x283	HSS10x0.375	W18x65
5	W14x283	HSS10x0.375	W18x35
4	W14x398	HSS9-5/8x0.5	W18x71
3	W14x398	HSS9-5/8x0.5	W18x35
2	W14x550	HSS9-5/8x0.5	W18x71
1	W14x550	HSS9-5/8x0.5	W18x35

Table A1.10: Member Sizes for 16 story SCBF building

Story	Columns	Braces	Beams
16	W12x45	HSS9-5/8x0.375	W18x65
15	W12x45	HSS9-5/8x0.375	W18x35
14	W14x82	HSS8-5/8x0.5	W18x71
13	W14x82	HSS8-5/8x0.5	W18x35
12	W14x120	HSS11-1/4x0.5	W18x86
11	W14x120	HSS11-1/4x0.5	W18x35
10	W14x176	HSS10x0.625	W18x86
9	W14x176	HSS10x0.625	W18x35
8	W14x233	HSS11-1/4x0.625	W18x97
7	W14x233	HSS11-1/4x0.625	W18x35
6	W14x283	HSS11-1/4x0.625	W18x97
5	W14x283	HSS11-1/4x0.625	W18x35
4	W14x342	HSS11-1/4x0.625	W21x93
3	W14x342	HSS11-1/4x0.625	W18x35
2	W14x370	W12x96	W24x146
1	W14x370	W12x96	W18x35

A.2 Summary of Ground Motions

Table A2.1: Summary of 30 Strike Slip- Ground Motions

GM No	Earthquake Name	Year	Station Name	Magnitude	Rrup (km)	PGA (g)			
						Horizontal 1	Horizontal 2	Vertical	V/H
1	"Erzican_ Turkey"	1992	"Erzincan"	6.69	4.38	0.50	0.39	0.23	0.47
2	"Kobe_ Japan"	1995	"KJMA"	6.9	0.96	0.83	0.63	0.34	0.41
3	"Kobe_ Japan"	1995	"Takarazuka"	6.9	0.27	0.70	0.61	0.43	0.61
4	"Denali_ Alaska"	2002	"TAPS Pump Station #10"	7.9	2.74	0.33	0.30	0.24	0.72
5	"Tottori_ Japan"	2000	"SMNH01"	6.61	5.86	0.62	0.73	0.64	0.87
6	"Tottori_ Japan"	2000	"TTRH02"	6.61	0.97	0.77	0.94	0.79	0.84
7	"Bam_ Iran"	2003	"Bam"	6.6	1.7	0.81	0.63	0.97	1.20
8	"Darfield_ New Zealand"	2010	"GDLC"	7	1.22	0.76	0.71	1.25	1.63
9	"Darfield_ New Zealand"	2010	"HORC"	7	7.29	0.45	0.48	0.81	1.70
10	"Kobe_ Japan"	1995	"Nishi-Akashi"	6.9	7.08	0.48	0.46	0.39	0.80
11	"Duzce_ Turkey"	1999	"Lamont 1058"	7.14	0.21	0.11	0.08	0.07	0.69
12	"Duzce_ Turkey"	1999	"Lamont 1059"	7.14	4.17	0.14	0.15	0.10	0.66
13	"Duzce_ Turkey"	1999	"IRIGM 487"	7.14	2.65	0.28	0.30	0.23	0.76
14	"Imperial Valley-06"	1979	"Agrarias"	6.53	0.65	0.29	0.19	0.47	1.64
15	"Imperial Valley-06"	1979	"Bonds Corner"	6.53	2.66	0.60	0.78	0.53	0.68
16	"Imperial Valley-06"	1979	"Chihuahua"	6.53	7.29	0.27	0.25	0.22	0.80
17	"Imperial Valley-06"	1979	"EC County Center FF"	6.53	7.31	0.21	0.24	0.24	1.04
18	"Imperial Valley-06"	1979	"El Centro Array #5"	6.53	3.95	0.53	0.38	0.59	1.12
19	"Imperial Valley-06"	1979	"El Centro Array #6"	6.53	1.35	0.45	0.45	1.90	4.22
20	"Imperial Valley-06"	1979	"El Centro Array #7"	6.53	0.56	0.34	0.47	0.58	1.23
21	"Imperial Valley-06"	1979	"El Centro Array #8"	6.53	3.86	0.61	0.47	0.47	0.77
22	"Imperial Valley-06"	1979	"El Centro Differential Array"	6.53	5.09	0.35	0.48	0.77	1.60
23	"Imperial Valley-06"	1979	"Holtville Post Office"	6.53	7.5	0.26	0.22	0.26	1.00
24	"Kobe_ Japan"	1995	"Port Island (0 m)"	6.9	3.31	0.35	0.29	0.57	1.63
25	"Kocaeli_ Turkey"	1999	"Yarimca"	7.51	4.83	0.23	0.32	0.24	0.75
26	"Duzce_ Turkey"	1999	"Duzce"	7.14	6.58	0.40	0.51	0.35	0.67
27	"Darfield_ New Zealand"	2010	"DSLC"	7	8.46	0.26	0.24	0.32	1.23
28	"Darfield_ New Zealand"	2010	"LINC"	7	7.11	0.46	0.39	0.91	1.98
29	"Darfield_ New Zealand"	2010	"ROLC"	7	1.54	0.39	0.32	0.71	1.82
30	"Darfield_ New Zealand"	2010	"TPLC"	7	6.11	0.30	0.21	0.87	2.92

Table A2.2 - Summary of 30 Reverse Fault- Ground Motions

GM No	Earthquake Name	Year	Station Name	Magnitude	Rrup (km)	PGA (g)			
						Horizontal 1	Horizontal 2	Vertical	V/H
1	"Northridge-01"	1994	"Jensen Filter Plant Administrative Building"	6.69	5.43	0.41	0.62	0.35	0.56
2	"Northridge-01"	1994	"Pardee - SCE"	6.69	7.46	0.56	0.30	0.39	0.69
3	"Northridge-01"	1994	"Sylmar - Converter Sta East"	6.69	5.19	0.85	0.45	0.48	0.56
4	"Northridge-01"	1994	"Sylmar - Olive View Med FF"	6.69	5.3	0.60	0.84	0.54	0.64
5	"San Simeon_ CA"	2003	"Cambria - Hwy 1 Caltrans Bridge"	6.52	7.25	0.18	0.13	0.09	0.49
6	"San Simeon_ CA"	2003	"Templeton - 1-story Hospital"	6.52	6.22	0.44	0.48	0.26	0.55
7	"Niigata_ Japan"	2004	"NIG019"	6.63	9.88	1.33	1.17	0.80	0.60
8	"Niigata_ Japan"	2004	"NIG020"	6.63	8.47	0.41	0.53	0.31	0.59
9	"Niigata_ Japan"	2004	"NIG028"	6.63	9.79	0.52	0.85	0.44	0.52
10	"Niigata_ Japan"	2004	"NIGH01"	6.63	9.46	0.67	0.84	0.38	0.45
11	"Niigata_ Japan"	2004	"NIGH11"	6.63	8.93	0.60	0.46	0.32	0.53
12	"Montenegro_ Yugoslavia"	1979	"Bar-Skupstina Opstine"	7.1	6.98	0.37	0.37	0.24	0.65
13	"Montenegro_ Yugoslavia"	1979	"Ulcinj - Hotel Albatros"	7.1	4.35	0.18	0.23	0.23	0.99
14	"Montenegro_ Yugoslavia"	1979	"Ulcinj - Hotel Olimpic"	7.1	5.76	0.29	0.25	0.46	1.57
15	"Tabas_ Iran"	1978	"Tabas"	7.35	2.05	0.85	0.86	0.64	0.74
16	"Nahanni_ Canada"	1985	"Site 1"	6.76	9.6	1.11	1.20	2.28	1.90
17	"Nahanni_ Canada"	1985	"Site 3"	6.76	5.32	0.18	0.17	0.14	0.79
18	"Cape Mendocino"	1992	"Cape Mendocino"	7.01	6.96	1.49	1.04	0.74	0.49
19	"Northridge-01"	1994	"Jensen Filter Plant Generator Building"	6.69	5.43	0.57	0.99	0.76	0.77
20	"Northridge-01"	1994	"LA Dam"	6.69	5.92	0.43	0.32	0.32	0.75
21	"Northridge-01"	1994	"Pacoima Kagel Canyon"	6.69	7.26	0.30	0.43	0.17	0.39
22	"Montenegro_ Yugoslavia"	1979	"Petrovac - Hotel Olivia"	7.1	8.01	0.46	0.30	0.21	0.45
23	"Iwate_ Japan"	2008	"IWTH25"	6.9	4.8	1.43	1.15	3.84	2.68
24	"Gazli_ USSR"	1976	"Karakyr"	6.8	5.46	0.70	0.86	1.70	1.97
25	"Northridge-01"	1994	"Arleta - Nordhoff Fire Sta"	6.69	8.66	0.35	0.31	0.55	1.60
26	"Northridge-01"	1994	"Newhall - Fire Sta"	6.69	5.92	0.58	0.59	0.55	0.93
27	"Northridge-01"	1994	"Newhall - W Pico Canyon Rd."	6.69	5.48	0.42	0.36	0.30	0.71
28	"Northridge-01"	1994	"Rinaldi Receiving Sta"	6.69	6.5	0.87	0.47	0.96	1.10
29	"Northridge-01"	1994	"Sylmar - Converter Sta"	6.69	5.35	0.62	0.92	0.61	0.66
30	"Iwate_ Japan"	2008	"IWT011"	6.9	8.44	0.22	0.15	0.21	0.96

BIBLIOGRAPHY

American Institute of Steel Construction (AISC) (2011). *Steel Construction Manual,* 4th Edition, Chicago, IL.

American Society of Civil Engineers (ASCE) (2016). *Minimum Design Loads for Buildings and Other Structures*. ASCE/SEI Standard 7-16.

American Society of Civil Engineers (ASCE) (2010). *Minimum Design Loads for Buildings and Other Structures*. ASCE/SEI Standard 7-10.

Baker, J.W. (2007). "Probabilistic structural response assessment using vector valued intensity measures". *Earthquake Engineering and Structural Dynamics*; 36(5):1861-83.

Bozorgnia, Y.N., and Campbell, K.W. (1995). "Characteristics of free field vertical ground motion during the Northridge earthquake". *Earthquake Spectra*; 11(4):515-525.

Bozorgnia, Y.N., and Campbell, K.W. (2003). "The vertical-to-horizontal response spectral ratio and tentative procedures for developing simplified V/H and vertical design spectra". *Journal of Earthquake Engineering; 8(2):175-207.*

Bozorgnia, Y.N., and Campbell, K.W. (2016). "Ground Motion Model for the Vertical-to-Horizontal (V/H) Ratios of PGA, PGV, and Response Spectra". *Earthquake Spectra*; Vol. 32, No. 2, pp. 951-978.

Bozorgnia, Y.N., and Campbell, K.W. (2016). *"*Vertical Ground Motion Model for PGA, PGV, and Linear Response Spectra Using the NGA-West2 Database". *Earthquake Spectra*; Vol. 32, No. 2, pp. 979-1004.

Collier, C. J., and Elnashaia, A. S. (2001). *"*Procedure for Combining Vertical and Horizontal Seismic Action Effects*". Journal of Earthquake Engineering*; Volume 5- Issue 4.

Cornell, C. A., Jalayer, F., Hamburger, R. O., and Douglas A. F. (2002). "Probabilistic Basis for 2000 SAC Federal Emergency Management Agency Steel Moment Frame Guidelines". *Journal of Structural Engineering*; Volume 128 Issue 4.

Der Kiureghian, A., and Liu, P.L. (1986) "Structural Reliability under Incomplete Probability Information". *Journal of Engineering Mechanics*; Vol. 112 Issue 1.

Ebrahimi, S. (2016). "Effect of Vertical Component of Ground Motion on Dual System Tall Buildings". *MS Thesis*; University of California, Irvine, CA.

Ellingwood, B., Galambos, T. V., MacGregor, J. G., and Cornell, C.A. (1980). "Development of a Probability Based Load Criterion for American National Standard A58".

Elnashai, A. S., and Papazoglou, A. J. (2004). "Procedure and Spectra for Analysis of RC Structures Subjected to Strong Vertical Earthquake Loads". *Journal of Earthquake Engineering*; Volume 8- Issue 5.

FEMA 2009. "Quantification of Building Seismic Performance Factors", *FEMA P695*, Prepared by the Applied Technology Council (ATC), Federal Emergency Management Agency (FEMA), *NIST GCR 10-917-8*- Washington DC,

Hasofer, A. M., and Lind, M. C. (1974). *"*An Exact and Invariant First Order Reliability Format". *Journal of Engineering Mechanics;* Vol. 100, 1974, pp. 111-121.

Jalayer, F. C., and Cornell C.A. (2003). "A technical framework for probability-based demand and capacity factor (DCFD) seismic formats". PEER Report 2003/08; Pacific Earthquake Engineering Center, University of California, Berkeley, CA.

Kim, S.J., Holub, C.J., and Elnashai, A.S. (2011). "Analytical assessment of the effect of vertical earthquake." *Journal of Structural Engineering;* 137(2):252-260

Luco, N., and Cornell, C.A. (1998). "Effects of random connection fractures on the demands and reliability for a 3-story pre-Northridge SMRF structure". *Proc., 6th U.S. National Conference on Earthquake Engineering*; Earthquake Engineering Research Institute, Oakland, CA.

Luco, N., and Cornell, C.A. (2000). "Effects of connection fractures SMRF seismic drift Demands". *Journal of Structural Engineering*; 126(1),127-136

Luco, N., Ellingwood, B.R., Hamburger, R.O., Hooper, J.D., Kimball, J.K., and Kircher, C.A. (2007). "Risk-Targeted versus Current Seismic Design Maps for the Conterminous United States". SEAOC 2007 Convention, Proceedings, vol. 1, 2007;163-175.

Melchers, R. E. (1999), *Structural Reliability Analysis and Prediction*. Second Edition, John Wiley & Sons; ISBN 0-471-98771-9

Naeim, F. (2001). *The Seismic Design Handbook*, Second Edition, Springer; ISBN-10: 0792373014.

Newmark, N. M., Blume, J. A., and Kapur, K. (1973). "Seismic design spectra for Nuclear Power Plants". *Journal of the Power Division*; 99(2):287-303.

Shome, N. and Cornell, C. A. (1999). "Probabilistic seismic demand analysis of nonlinear Structures". Rep NO. RMS-35, Stanford University, Stanford, CA

Sashi, K. K., Emrah, E., Chai, Y. H., and Yashinsky, M. (2008). "Effect of Near-Fault Vertical Ground Motions on Seismic Response of Highway Overcrossings". *Journal of Bridge Engineering*; Volume 13 Issue 3.

Thoft-Christensen, P., Baker, M. J. (1982). "Structural Reliability Theory and its Applications". Springer Berlin Heidelberg; ISBN- 978-3-642-68697-9

Timothy, D. A., Robert, B. D., Jonathan, P. S., Emel, S., Walter, J. S., Brian, S., Chiou, J., Wooddell, K. E., Graves, R. W., Kottke, A. R., Boore, D. M., Kishida, T., and Donahue, J. L., (2014). "NGA-West2 Database". *Earthquake Spectra*; August 2014, Vol. 30, No. 3, pp. 989-1005.

Vamvatsikos, D. (2012). “Derivation of new SAC/FEMA performance evaluation solutions with second-order hazard approximation”. *Earthquake Engineering and Structural Dynamics*; Vol. 42, Issue 8, pp. 1171-1188

Wen, Y. K. (1995). “Building Reliability and Code Calibration”. *Earthquake Spectra;* Vol. 11, No. 2, pp. 269-296.

Zareian, F. and Kanvinde, A. (2013). “Effect of Column-Base Flexibility on the Seismic Response and Safety of Steel Moment-Resisting Frames”. *Earthquake Spectra*; Vol. 29, No. 4, pp. 1537-1559.